Electronic supplementary materials *Mendeleev Commun.*, 2022, **32**, 510–513

Effect of textural characteristics on the catalytic performance of supported $KCoMoS_2$ in the synthesis of higher alcohols from syngas

Mohamed E. Osman, Vladimir V. Maximov, Tshepo D. Dipheko, Tatiana F. Sheshko, Alexander G. Cherednichenko and Victor M. Kogan

Experimental details All supports and supported catalysts were crushed and sieved to obtain powders with particle size in the 0.2-0.5 mm range. Carbon-coated alumina was prepared by pyrolysis according to the method described in [G. D. Yadav and S. B. Kamble, *Ind. Eng. Chem. Res.* 2009, 48, 21, 9383]; the carbon content (wt. %) was characterized by thermal gravimetric analysis (TGA) using a NETZSCH STA 4449 F3 Jupiter device. Powdered AC (AG-3) was produced from crude soft coking coal and semi-coke coal with coal. AC BAW was produced from patchy-shaped charcoal gravel obtained by gas-vapor activation at 850-950°C. The catalysts were prepared by wetness impregnation using the following precursors: $(NH4)_6Mo_7O_{24} \cdot 4H_2O$ (5 mmol), $Co(OAc)_2 \cdot 4\ H_2O$ (2.5 mmol), and KOH. A mixture of ammonia solution (20%, 2 ml) and deionized water (1.5 ml) was prepared. Ammonium heptamolybdate tetrahydrate was weighed and dissolved in the mixture. Also, potassium hydroxide (10 mmol) was dissolved in the mixture. The first mixture was transferred into a mixture of cobalt acetate tetrahydrate (2.5 mmol) and citric acid (5 mmol) in deionized water (1 ml). The final mixture was impregnated on microporous and mesoporous supports. The synthesized supported catalysts were dried for 2 h at 80 °C and then for 5 h at 105 °C. Sulfurization of the sup-$KCoMoO_4$ catalysts was performed using elemental sulfur (1:4, catalyst/sulfur) in an autoclave at 365 °C under hydrogen for 1 h at 6.0 MPa. Table S1 summarizes data on the targeted and measured composition of the catalysts determined by X-ray fluorescence (XRF, Shimadzu, Kyoto, Japan). The sup-KCoMoS catalysts are abbreviated as Cat-Al_2O_3, Cat-CCA, Cat-AG-3, and Cat-BAW, where Cat denotes $KCoMoS_2$ catalysts.

The surface properties were characterized using Quantachrome Nova 1200e and N_2 adsorption-desorption isotherms at 77 K were recorded. BET equation was used to calculate SSA. The total pore volume was determined at $P/P_o = 0.99$. To calculate pore size distribution and volume, the Barrett-Joyner-Halenda (BJH) method was used. The micropore volume of sample 20 was calculated from total and mesopore volumes.

The surface morphology of both supports and catalysts was studied using a Hitachi SU8000 Field-Emission Scanning Electron Microscope (FE-SEM). The samples were mounted on 25 mm aluminum specimen stubs using a conductive adhesive tape. Uncoated samples were studied to

avoid metal coating surface effects. Secondary electron images were recorded at the 10 kV accelerating voltage and the 8-10 mm working distance. By using an energy dispersive X-ray spectrometer Oxford Instruments X-max 80 at the accelerating voltage of 20 kV, the catalysts were characterized based on the X-ray microanalysis method (EDS-SEM) on an electron microscope Hitachi SU-8000.

A LaB6 Tecnai G2 20F Transmission Electron Microscope (TEM) operated at 200 kV and a LaB6 Tecnai G2 30F TEM operated at 300 kV were used to characterize the morphology of the sulfided catalysts.

Acid-base properties of the supported catalysts were analyzed using UV spectra of pyridine adsorption. The concentration in the solutions was determined by UV spectra using a SF-103 single-beam scanning spectrophotometer. The adsorption spectra of pyridine in the UV region of the blank pyridine solution in octane and solutions of adsorption systems with the supports and catalysts were recorded at ambient temperature for 60 min. The absorption maximum is in the region of 253 nm (analytical absorption band) and does not shift as the pyridine concentration varies. The concentration of the tested catalysts was determined by the calibration curve plotted between the optical density of the solution D and the pyridine concentration. Gibbsian adsorption (G, mol/g) was calculated using Eq. S1:

$$G = \frac{(\mathrm{C}_0 - \mathrm{C}_t) \times V}{m} = \frac{(D_0 - D_t) \times V}{m \times \varepsilon \times l} \qquad \text{(Eq: S1)}$$

where V is the volume of the solution (10 ml); m is the mass of the sample (0.1 g); D_0 and D_t are the optical density at the pyridine absorption maximum before and during adsorption; l is the thickness of the cuvette (1 cm); ε is the molar absorption coefficient (extinction, ε of pyridine = 2,106 $dm^3/(mol \cdot cm)$, εBac = 1,104 $dm^3/(mol \cdot cm)$).

Alcohols were synthesized from syngas using a tubular flow reactor with a (HAS) catalytic system. The sup-$KCoMoS_2$ catalyst (3 g) was weighed and loaded into the system under the following conditions: P = 5.0 MPa, temperatures = 300, 320, 340 and 360 ºC, volume ratio of the synthesis gas components [$CO/H_2/Ar$ = 45%:45%:10%, weight space velocity (GHSV=460 h^{-1}, catalyst loading 3 g)]. Argon was used as an internal standard carrier gas for gas chromatography. The experiment was conducted for 4h at each temperature (summary 16 h) at T = 300–360 °C (starting from 300 ºC with a 20 ºC step). The gaseous products were analyzed every 4h using a LHM-80 GC with a Thermal Conductivity Detector (TCD) and two 1 m packed columns (molecular sieves CaA (Ar, CH_4, CO) and Porapak Q (CO_2, C2+)). Liquid products were collected after 16 h and analyzed by a FID-GC detector on 25 m OV-101 and 25 m terephthalic acid/polyethylene glycol columns. CO conversion (CO (X)) was calculated using Eq. S2.

Selectivity in this reaction was calculated in the CO_2-free basis approximation since CO_2 is mainly formed in the course of the water-gas shift or Boudouard reactions and is considered as a byproduct that constantly affects selectivity of target products, which is why CO_2 was excluded from the selectivity balance calculations. Selectivities for free CO_2 were determined according to Eq. S3.

$$X_C(\%) = 1 - \frac{n_{CO}^{After\ reaction}}{n_{CO}^{In\ feed}} \times 100 \qquad \text{(Eq:S2)}$$

where X_C = syngas conversion and n_{CO}^{feed} and $n_{CO}^{Afterreaction}$ = CO content.

$$S_i^{CO_2-free}(\%) = \frac{S_i}{1 - S_{CO_2}} \times 100 \qquad \text{(Eq:S3)}$$

Table S1. Targeted and measured compositions of sup-$KCoMoS_2$ catalysts

Cat.	Targeted (wt. %)			Measured (wt. %)		
	K	Mo	Co	K	Mo	Co
Cat-Al_2O_3	10	12	3.7	10.2	15.8	5.1
Cat-CCA	10	12	3.7	11.6	14.4	4.7
Cat-AG-3	10	12	3.7	12.3	14.9	5.7
Cat-BAW	10	12	3.7	12.0	14.8	5.2

Table S2. Texture characteristics of supports and catalysts

Sample	SA_{total}, $m^2\ g^{-1}$	SA_{micro}, $m^2\ g^{-1}$	SA_{meso}, $m^2\ g^{-1}$	V_{total}, $cm^3\ g^{-1}$	V_{micro}, $cm^3\ g^{-1}$	V_{meso}, $cm^3\ g^{-1}$
Al_2O_3	161	0	161	0.65	0.00	0.65
CCA	156	13	143	0.63	0.01	0.63
AG-3	854	753	101	0.45	0.35	0.10
BAW	753	642	111	0.39	0.26	0.13
Cat-Al_2O_3	91	0	91	0.29	0.00	0.29
Cat-CCA	73	0	73	0.26	0.00	0.26
Cat-AG-3	164	137	27	0.09	0.06	0.03
Cat-BAW	404	365	40	0.23	0.16	0.07

Table S3. Selectivity for CH_4, and C_{2+} HCs, different alcohols, and CO_2 over supported KCoMoS2 catalysts

	C1 (%)	C2 (%)	MeOH (%)	EtOH (%)	PrOH (%)	Bu^iOH (%)	BuOH (%)	*i*-$C_5H_{11}OH$ (%)	*n*-$C_5H_{11}OH$ (%)	CO_2 (%)
Cat-Al_2O_3	4.9	1.1	8.6	17.7	17.7	11.1	6.6	4.6	2.9	24.8
Cat-CCA	4.5	0.5	9.1	18.2	17.9	12.5	8.0	4.9	3.6	22.1
Cat-AG-3	4.7	2.6	12.0	29.2	19.2	5.1	5.8	1.7	3.1	17.6
Cat-BAW	3.1	3.5	12.1	29.9	20.0	0	6.8	0.2	6.9	14.5

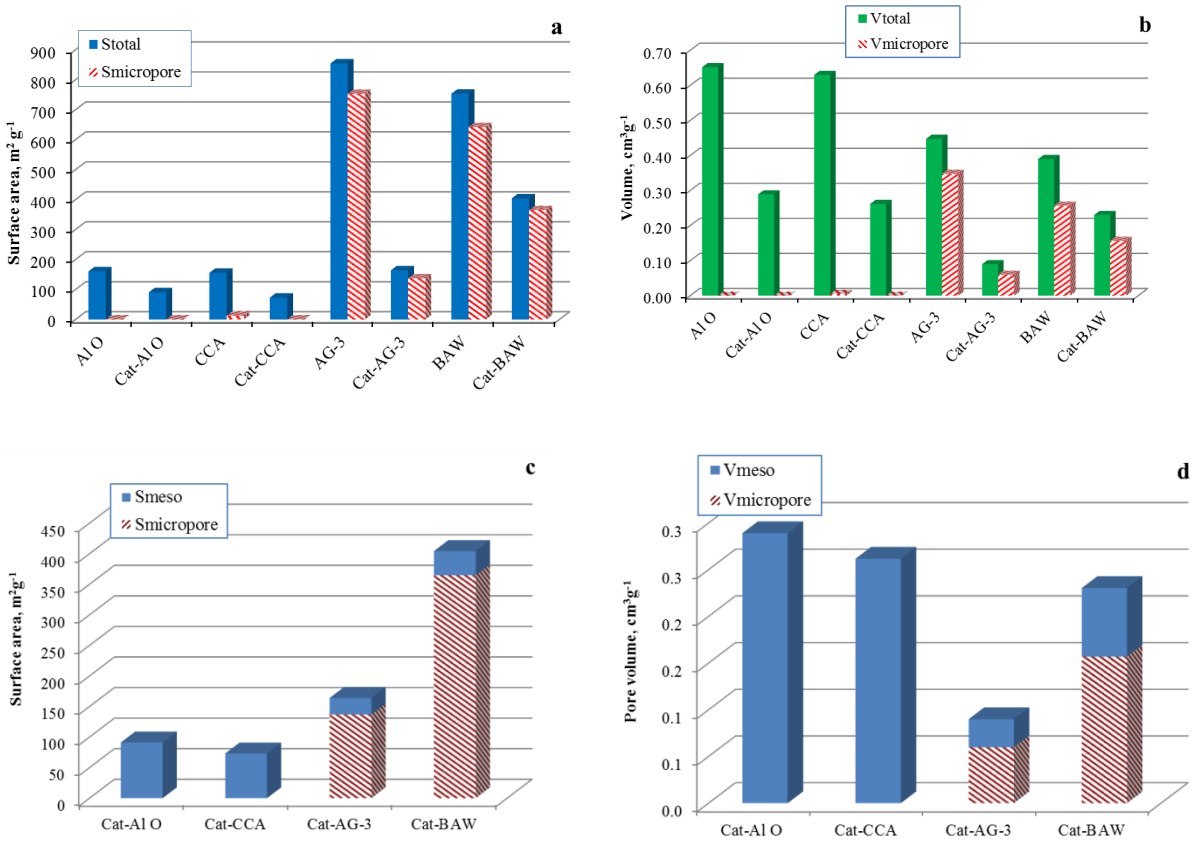

Figure S1 Specific surface areas of all the pores (S_{total}) and micropores ($S_{micropore}$) (***a***); total pore volume (V_{total}) and micropores volume ($V_{micropore}$) (***b***); distribution of macro + mesopores and micropores in the $KCoMoS_2$ catalysts supported on different carriers (Cat-carrier) for specific surface area (S_{meso}, $S_{micropore}$) (***c***) and for pore volume (V_{meso}, $V_{micropore}$) (***d***). The plots are color-coded.

Support name	SEM image of the support	SEM image of the supported-$KCoMoS_2$ catalyst
Al_2O_3	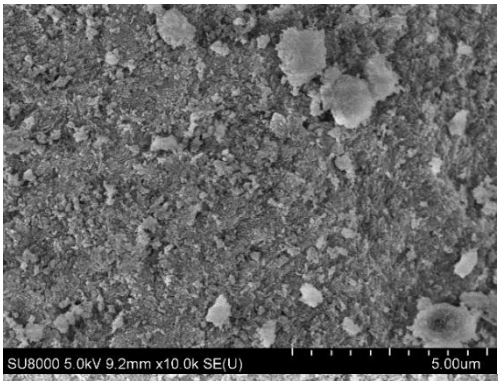	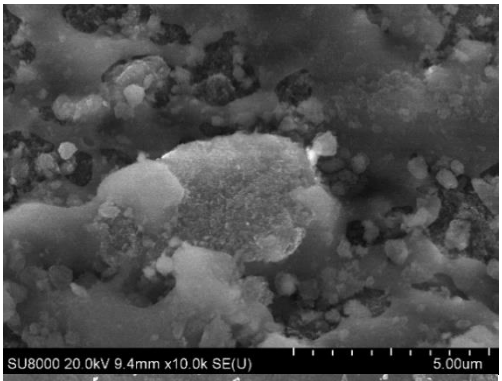
CCA	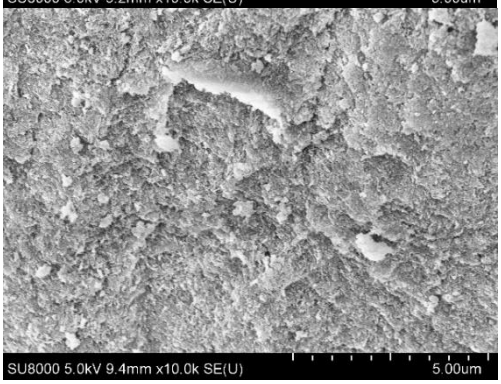	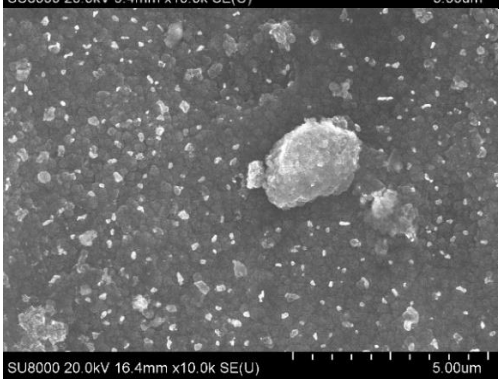
AG-3	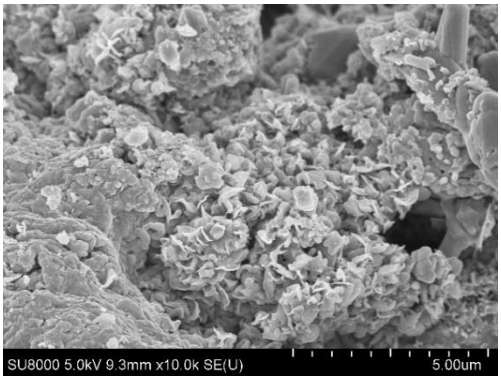	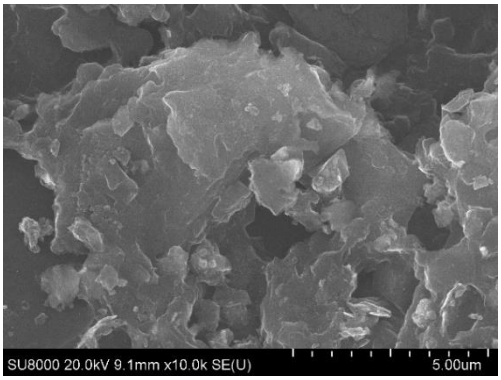
BAW	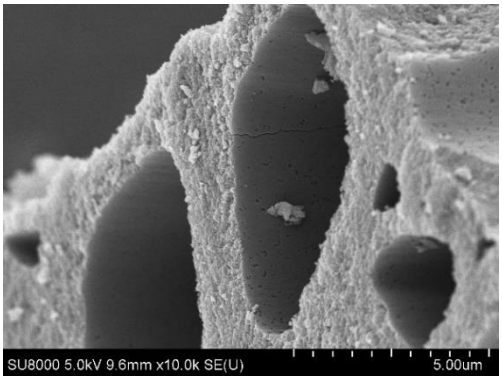	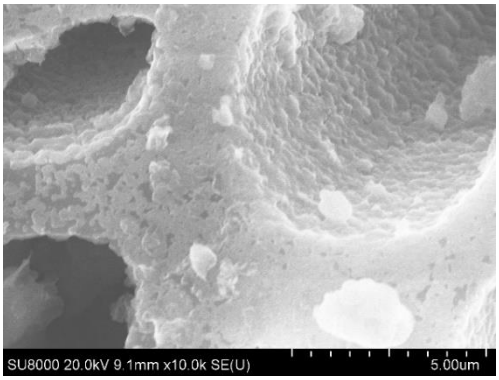

Figure S2. SEM images of the supports and the supported $KCoMoS_2$ catalysts.

Cat-Al_2O_3

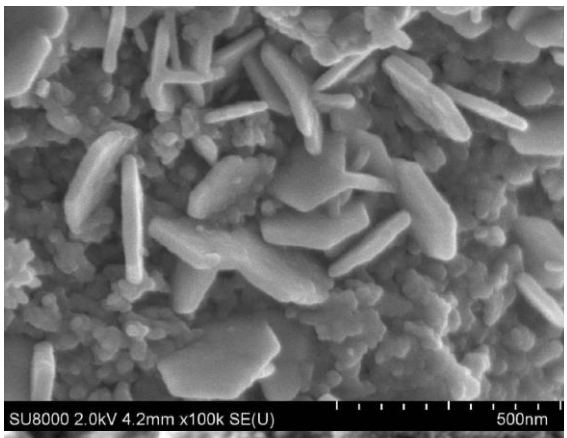

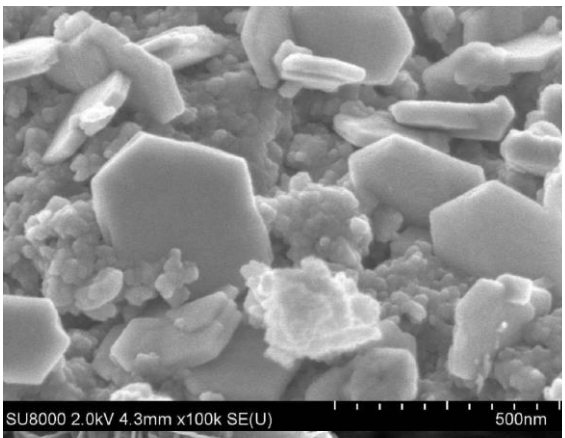

Cat-CCA

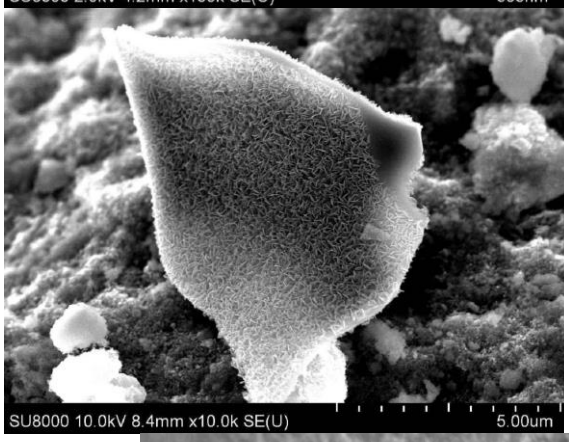

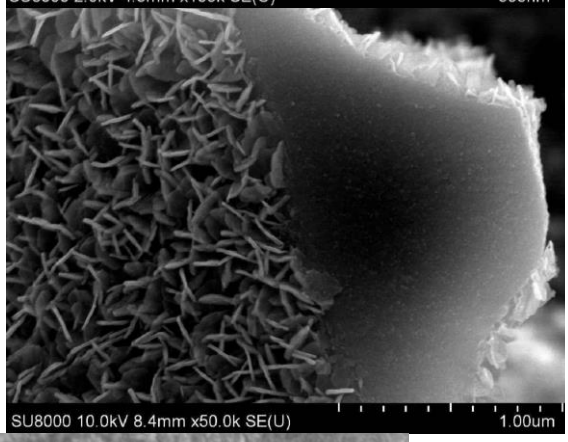

Cat-CCA

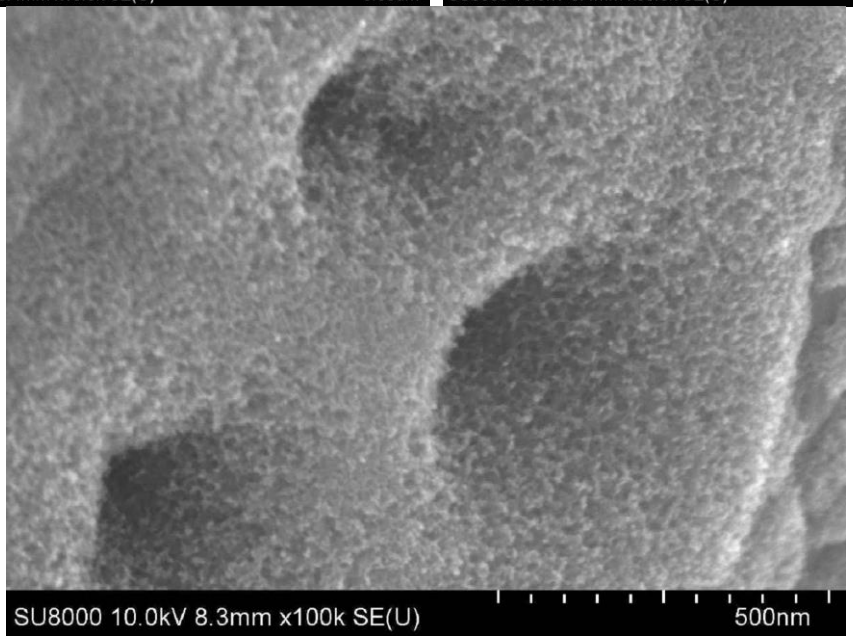

Figure S3. SEM images of giant agglomerations of $KCoMoS_2$ crystallites supported on mesoporous Al_2O_3 and CCA.

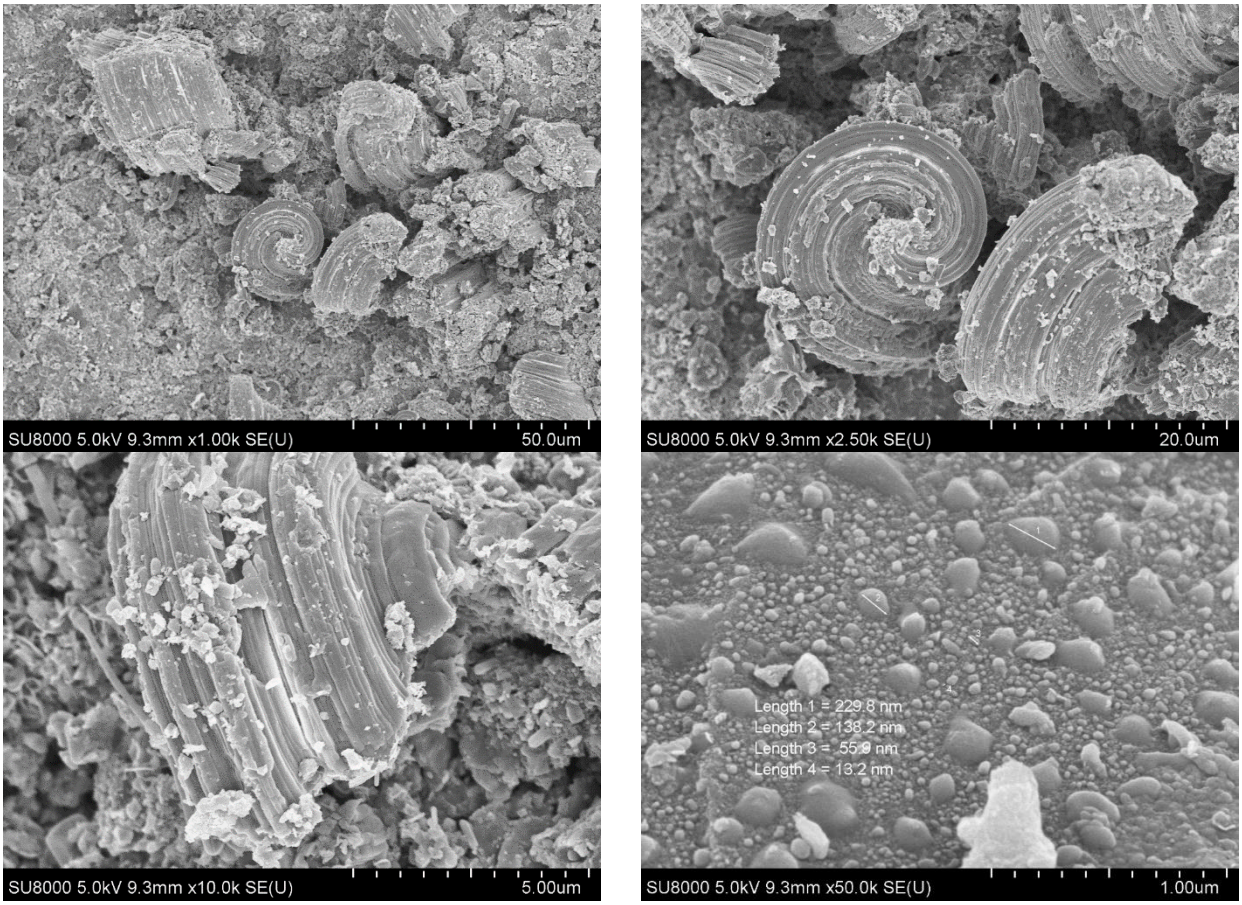

Figure S4. SEM images of the AG-3 support.

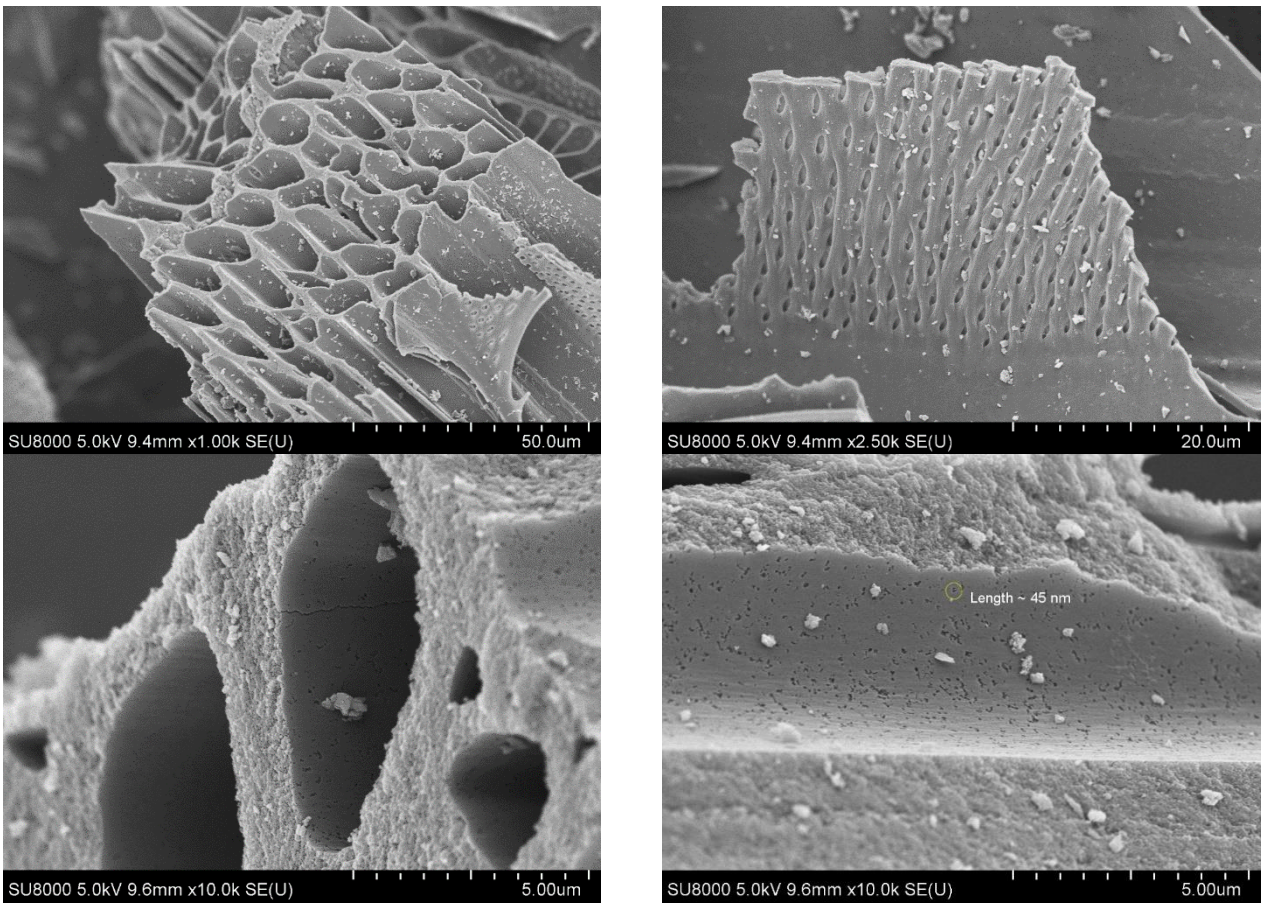

Figure S5. SEM images of the BAW support.

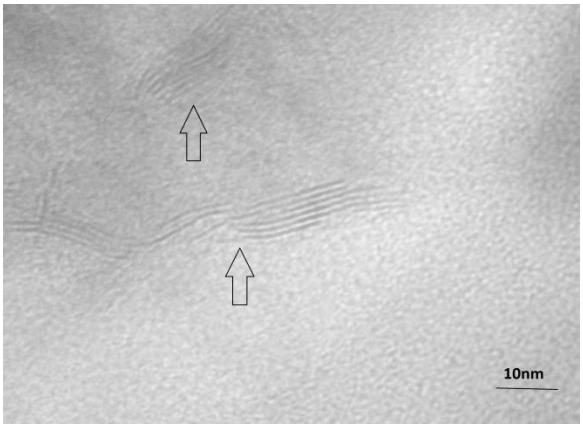

$KCoMoS_2/Al_2O_3$

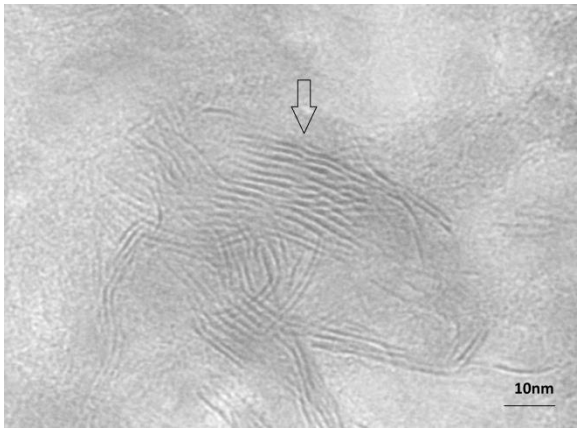

$KCoMoS_2$/CCA

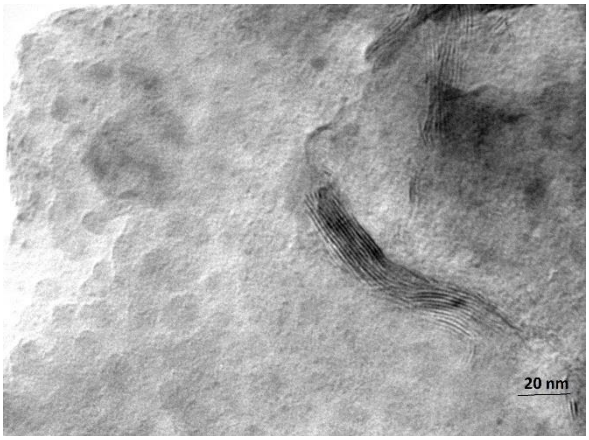

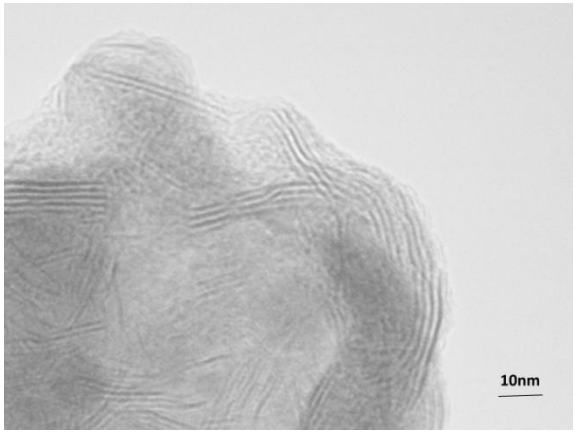

$KCoMoS_2$/AG-3 $KCoMoS_2$/BAW

Figure S6. TEM images of supported catalysts.

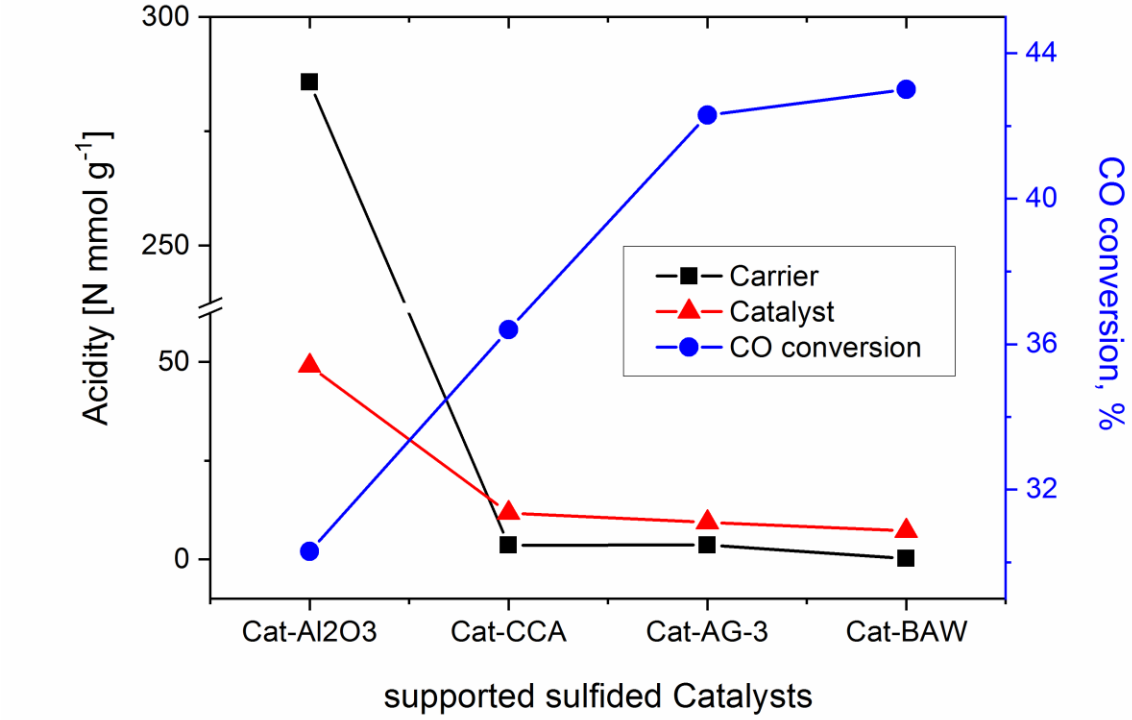

Figure S7. Acidity of supports and catalysts (black and red lines, respectively) and CO conversion dependence on acidity of catalysts (blue line).

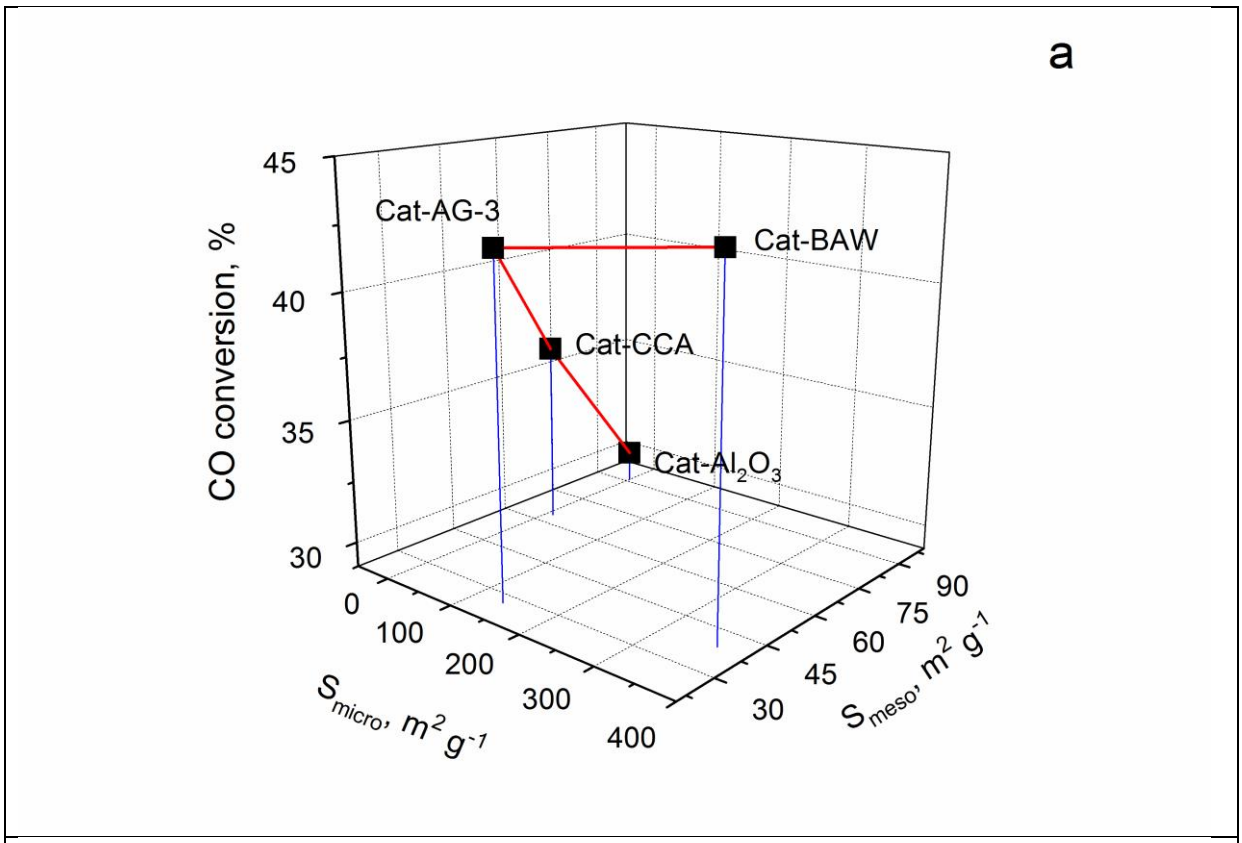

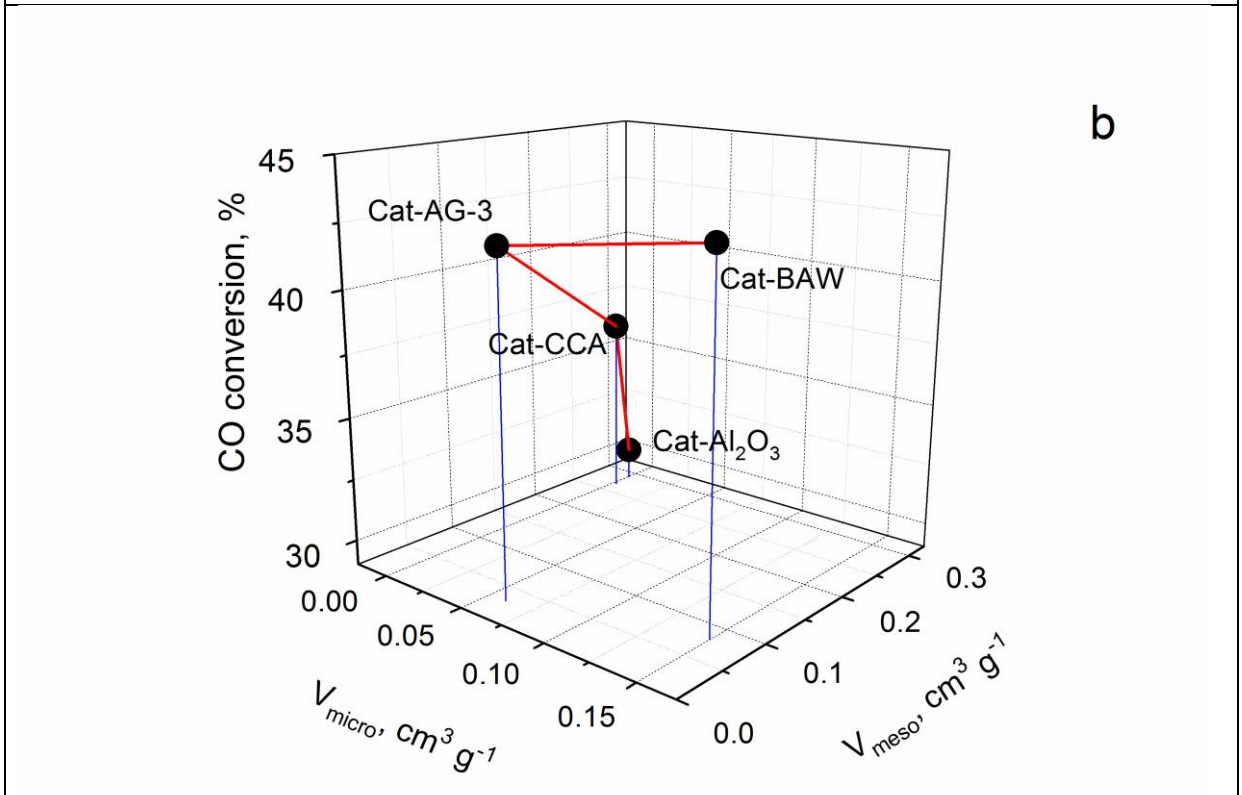

Figure S8. 3D plots of CO conversion, %, depending on (***a***) surface area of micro- (S_{micro}) and mesopores (S_{meso}), $m^2\ g^{-1}$, and (***b***) pore volume of micro- (V_{micro}) and mesopores (V_{meso}), $cm^3\ g^{-1}$.

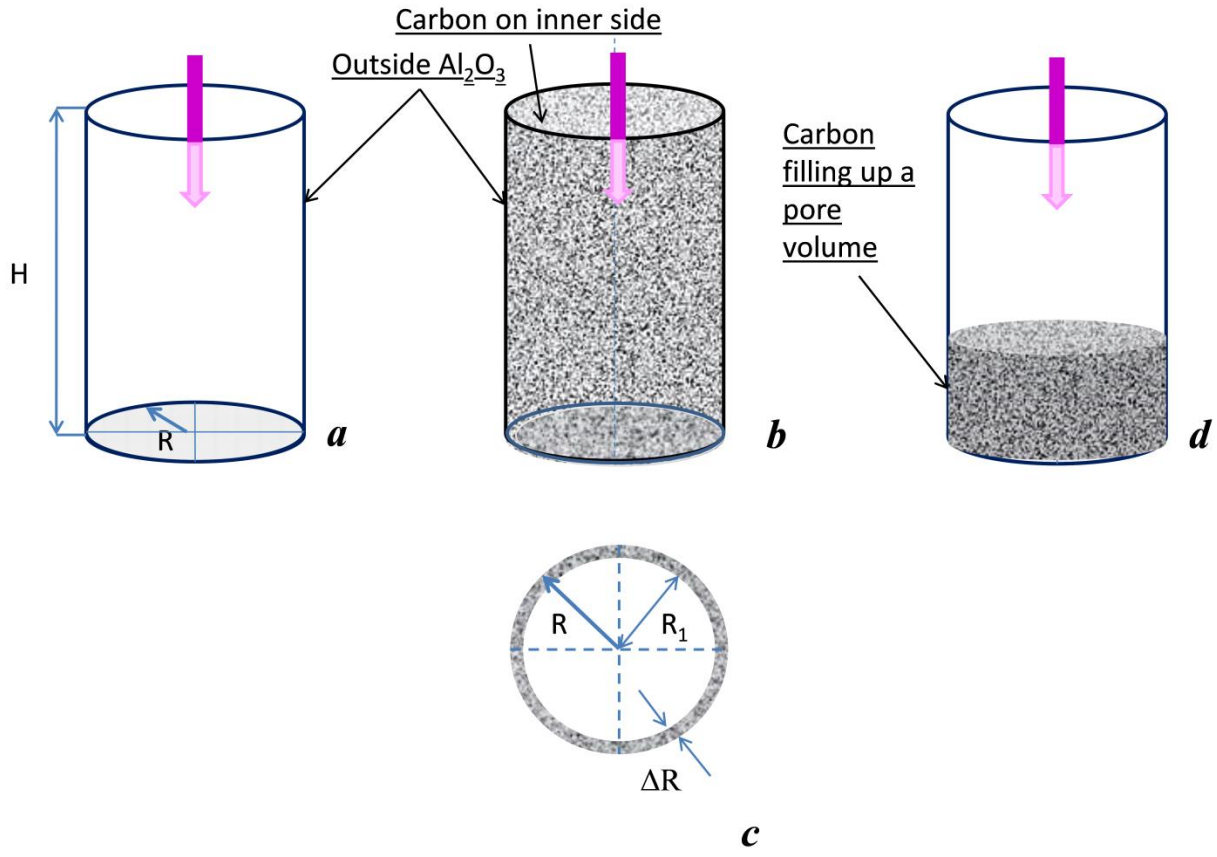

Figure S9. Simplified cylinder-type model of a mesopore in Cat-Al_2O_3 and Cat-CCA. (***a***) empty Al_2O_3 mesopore, side view; (***b***) mesopore with carbon deposited on the internal surface to form CCA, side view; (***c***) mesopore with carbon deposited on the internal surface to form CCA, top view; (***d***) amorphous carbon that fills part of the mesopore volume in CCA, side view.

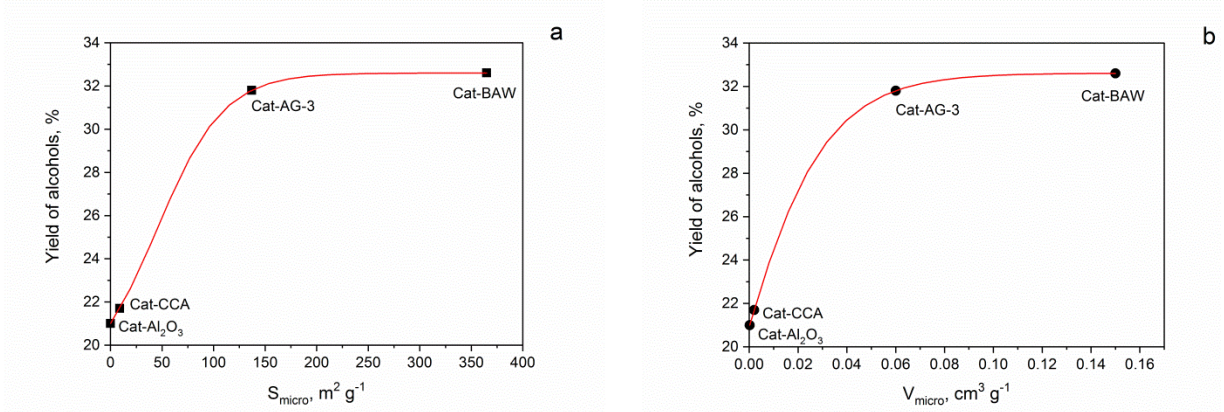

Figure S10. Dependences of alcohol yield on micropore specific surface area (S_{micro}) (***a***) and pore volume (V_{micro}) (***b***) at 360°C.

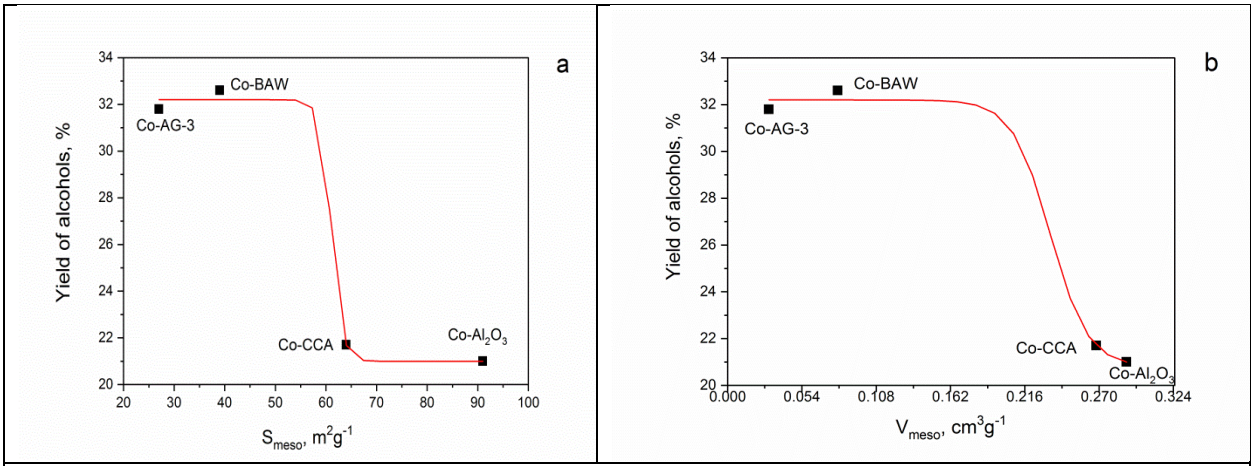

Figure S11. Dependences of alcohol yield on meso + macropores specific surface area (S_{micro}) (***a***) and pore volume (V_{micro}) (***b***) at 360°C.

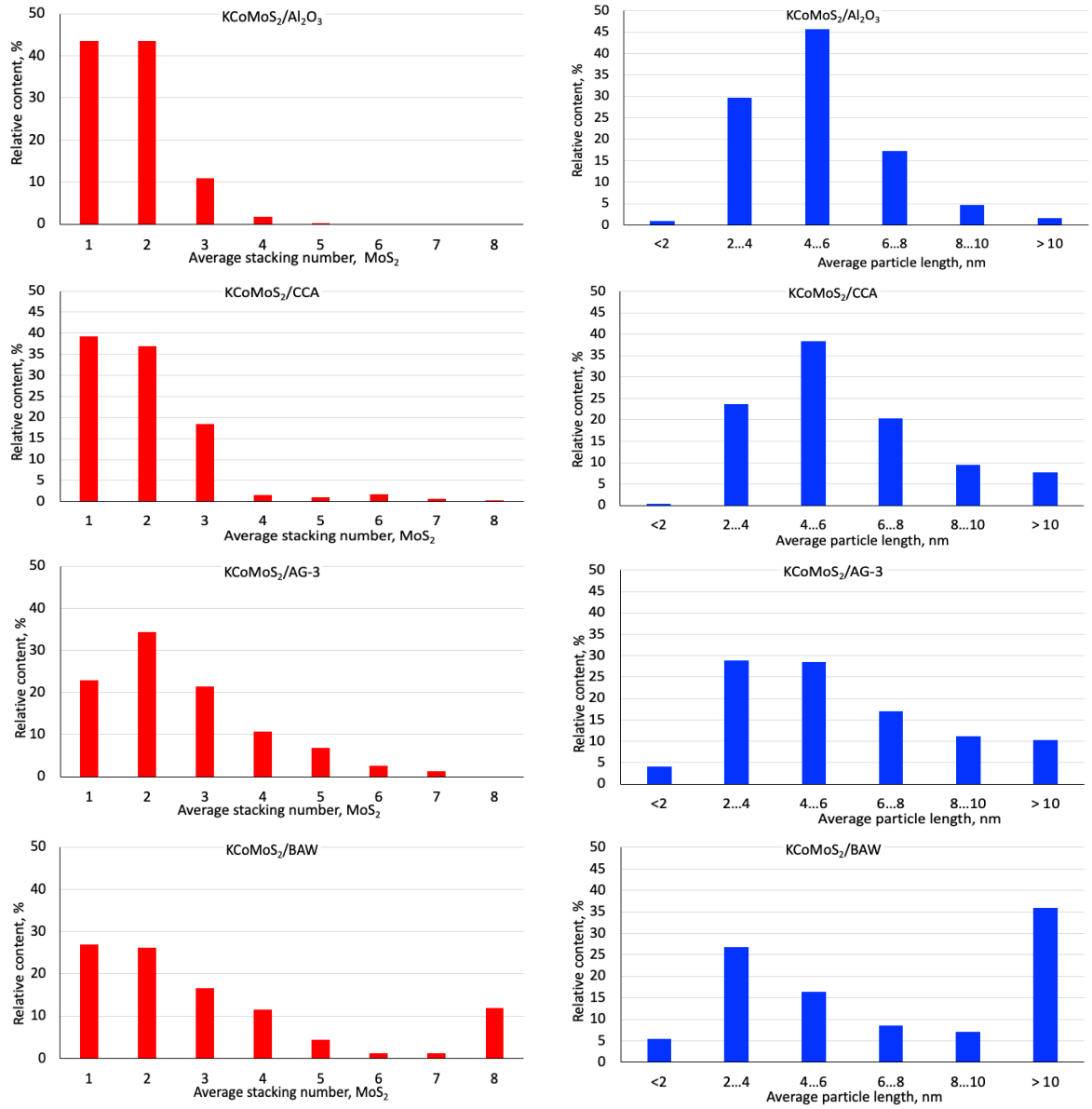

Figure S12. Distributions of slab lengths of MoS_2 particles and of stacking number of MoS_2 particles for sulfided catalysts.